

Enhanced Two-Photon Absorption and Ultrafast Dynamics of a New Multibranch Chromophore with a Dibenzothiophene Core

Yongli Yan,^{†,‡} Bo Li,^{†,‡} Kangjun Liu,^{†,‡} Zhiwei Dong,^{†,‡} Xiaomei Wang,[§] and Shixiong Qian^{*,†}

Physics Department, Fudan University, Shanghai 200433, People's Republic of China, Surface Physics Lab (National Key Lab), Fudan University, Shanghai 200433, People's Republic of China, and College of Material Science and Engineering, Suzhou University, Suzhou 215021, People's Republic of China

Received: November 22, 2006; In Final Form: February 10, 2007

A series of novel compounds with dibenzothiophene core branched structures have been synthesized, and their two-photon absorption (TPA) properties were investigated. Two-photon fluorescence (TPF) and z-scan techniques were carried out, and a significant enhancement in the TPA cross section was observed for ST-G2, which possesses the largest generation number among the studied samples. By using different solvents, the largest nonlinear optical (NLO) response was observed in the most polar solvent. Ultrafast pump–probe experiments were performed to probe the excited state dynamics in the branched molecules, and the obtained results further confirmed the TPA enhancement mechanism. Time-resolved fluorescence (TRFL) and TRFL anisotropy measurements reveal that there is an ultrafast charge localization to the intramolecular charge transfer (ICT) state followed by relaxation with a lifetime longer than 1 ns.

1. Introduction

Two-photon absorption, namely, the absorption of two photons simultaneously by the atoms or the molecules, has received much attention because of its huge potential applications in many innovative aspects such as three-dimensional micro-fabrication, laser technology, photodynamic therapy, optical limiting, optical data storage,^{1–7} and so on. Recently, abundant experimental and theoretical studies have been carried out to investigate the strategies for synthesis of organic molecules with large TPA cross sections. According to available results, a conclusion can be drawn that an electron-donor (D) and an electron-acceptor (A) symmetrically or asymmetrically joined through a π -bridge to form a linear D– π –A structure can effectively improve TPA activities and their strength for pushing and pulling electrons; the nature and length of the π -bridge as well as substituents are surely key factors for getting a large TPA cross section.^{8–11}

Constructing a multibranch structure is another attractive approach which can effectively enhance TPA performance.^{12–29} Because the enhancement of the TPA cross section is larger than the sum of that of each branch,^{17–21} the relationship between the structure and TPA property cannot be simply expressed as linear with the chromophore number density. However, a mechanism for explaining this phenomenon is still not very clear at present. Prasad et al. have reported that enhancement of the nonlinear optical (NLO) response in the trimer, compared to the monomers, is a factor of ~ 7 in the femtosecond time scale and ~ 10 in the nanosecond time scale.¹⁷ Drobizhev found that the peak TPA cross section increases quadratically with the number of chromophores in a dendrimer.¹⁹ Transient spectroscopy technology provides the capability for the further investigation of strong interactions among the

contributing chromophores in the dendritic structures. On the basis of many investigations aimed at understanding the factors which govern the NLO effect in branched molecules, intra-arm coupling, electron delocalization, and the extent of intramolecular charge transfer have been proposed.^{22–29} Recently, Peng et al. reviewed the synthesis and photophysical properties of dendrimers with unsymmetrical branching.³⁰ They show that unsymmetrical branching leads to stronger coupling of the perylene trap to the peripheral states.³⁰ However, these reported results are for a dendrimer containing a distyrylbenzene (DSB) unit as the core, where a nitrogen atom served as the center of the “three-arm” core. Multibranch molecules with other cores have not been studied.

In this manuscript, we report the results of NLO, TRFL, and transient absorption measurements of a series of new branched molecular structures with dibenzothiophene as the core and a triphenylamine unit as the “peripheral arm” (Figure 1). The smallest molecule ST-G1, whose core was flanked on both sides by one triphenylamine unit, is regarded as generation 1. ST-G1.5 and ST-G2, with ST-G1 as their cores, are regarded as generations 1.5 and 2, respectively, and the only difference is the branch number. A Ti:sapphire femtosecond laser system was employed to investigate the ultrafast dynamics to explore their structure/property relationships. An enhancement in the TPA cross section with the increasing generation number was observed. TRFL results show that the energy delocalization finishes in about 3 ps and their decay is greatly disturbed by the intramolecular interaction.

2. Experimental

2.1. Materials and Synthesis. All chemicals used in the synthesis and measurements, except the usual solvents and reagents, were purchased from Across Co. and were used without further purification. The detailed synthesis has been reported elsewhere.³¹ All synthesized compounds, presenting bright yellow color and being suitably soluble in common organic solvents, were purified by repeating chromatography

* Corresponding author. Tel: 86-21-65642084. Fax: 86-21-65641344. E-mail: sxqian@fudan.ac.cn.

[†] Physics Department, Fudan University.

[‡] Surface Physics Lab (National Key Lab), Fudan University.

[§] Suzhou University.

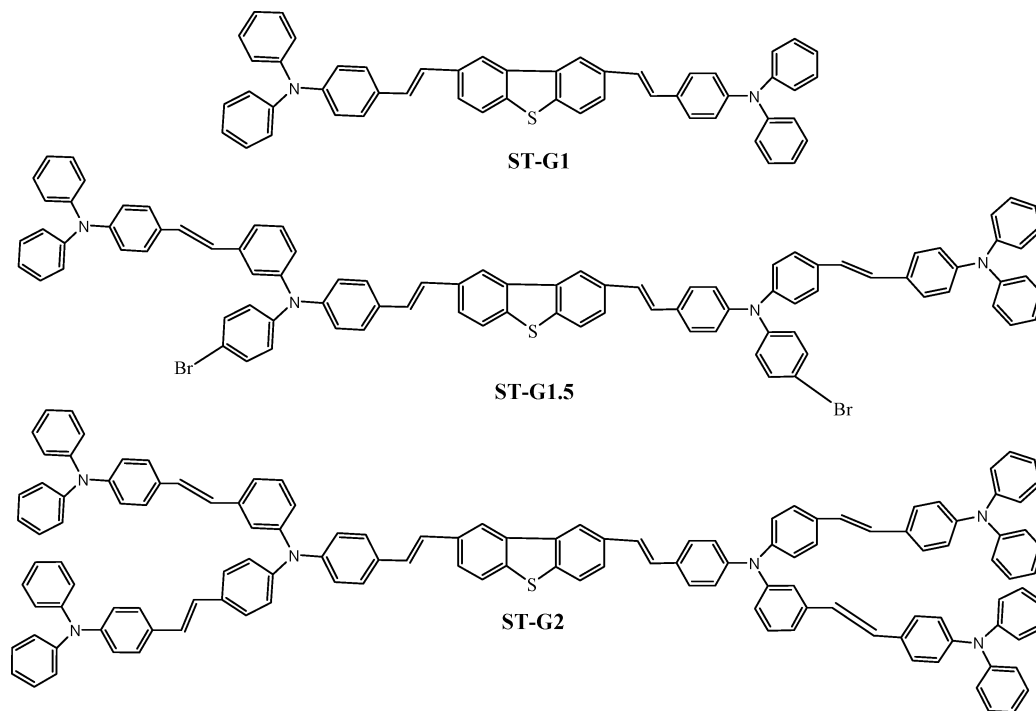


Figure 1. Chemical structures of three chromophores.

and confirmed by ^1H NMR spectra, electron impact (mode laser) mass spectra, and elemental analysis. Here, we used tetrahydrofuran (THF), *N,N*-dimethylformamide (DMF), and toluene to study solvent effects of these molecules.

2.2. Instruments and Measurements. Linear absorption spectra were measured with a spectrophotometer (Hitachi; U-3500) with 2 nm resolution. A quartz cuvette with a 1 mm path length was used for the dilute sample solutions. The influences from the quartz cell and the solvent have been subtracted. One-photon fluorescence spectra were measured by an Edinburgh FLS 920 fluorophotometer in a 1 cm path length cell. The concentration was 1.0×10^{-5} mol/L for linear absorption and fluorescence measurement, and solutions with a high concentration of 0.01 mol/L were used for NLO measurements. All experiments were performed at room temperature.

Our laser system was a Ti:sapphire regenerative amplifier (Spitfire, Spectra-Physics), operated at 1 kHz repetition rate and 140 fs pulse duration at 800 nm. The output femtosecond beam was used directly to pump sample solutions, and two-photon fluorescence (TPF) signals were collected in the direction perpendicular to the incident excitation beam by a spectrum analyzer.

An open-aperture *z*-scan technique³² was used to measure the NLO absorption coefficient and the TPA cross section. The laser pulses with an average output power of about 1 mW were focused on the solution in a 1 mm cell by a lens of 10 cm focal length, and after passing a bandpass filter the transmitted light was detected by a photodiode connected with a Boxcar integrator.

Pump–probe experiments were also carried out with a Ti:sapphire laser system centered at 800 nm. The fundamental output was split into pump and probe beams by a beam splitter. The pump beam was chopped using a chopper at a rate of 600 Hz and was focused onto a sample cell using an 8 cm focal length lens after passing through an optical delay line. The probe beam was focused to overlap with the pump beam on the same point in the sample cell by a lens with a focal length of 12 cm.

The pump beam was blocked by an aperture behind the sample. The modulated transmittance of the probe beam was measured by a photodiode and a lock-in amplifier (SR830, Stanford Research Systems), and the signal was finally recorded as a function of delay time on a computer. We inserted a quarter-wave plate and a polarizer in the path of the probe beam to change the polarization angle between the pump and probe beams. Therefore the pump–probe signals under different configurations (parallel, perpendicular, and magic-angle) could be obtained by rotating the polarizer.

A TRFL experimental setup utilizing the optical Kerr gate (OKG) technique³³ was discussed in our previous papers.²⁰ Briefly, the pump beam at 800 nm after passing an optical delay line was used as a gate beam to open the “Kerr gate” through photoinduced birefringence of Kerr material (CS_2), while the second part of the 800 nm beam was frequency-doubled by using a BBO crystal. The second harmonic pulses with vertical polarization were used to pump samples efficiently, and the collected fluorescence was set either parallel or perpendicular to that of the incident beam by a polarizer (P1). Another polarizer with orthogonal polarization to P1 was placed behind the sample to study the polarization effect. Dispersed by a monochromator, the signal was detected by a photomultiplier (Hamamatsu R1104) connected to a lock-in amplifier. The polarization of the gate beam was set at 45° with respect to that of SHG. In doing so, we can get TRFL signals under different configurations for anisotropy studies.

3. Results and Discussions

3.1. Absorption and Emission Spectra. Shown in Figure 2 are the linear absorption spectra and one-photon fluorescence spectra of the molecules in DMF, toluene, and THF, and the obtained data are given in Table 1. The absorption spectra of all three samples show broad band absorption with a shoulder located at about 300 nm which would be attributed to the absorption of the substituted phenyl.³¹ No obvious absorption is observed at a longer-wavelength region (>470 nm) in all cases. Interestingly, the absorption peaks show a gradual red-

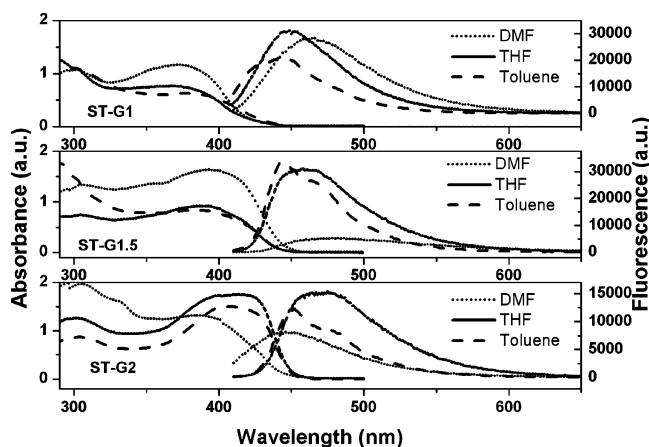


Figure 2. Linear absorption spectra and one-photon fluorescence spectra of sample solutions in DMF, THF, and toluene. From top to bottom: ST-G1, ST-G1.5, and ST-G2.

shift with increasing generation number, while the absorption shoulder remains the same. For example, there is a red-shift of the absorption peak of ST-G1.5 (390 nm) with respect to ST-G1 (368 nm), whereas the absorption peak of ST-G2 is even more red-shifted to 401 nm. These results strongly demonstrate that the interaction among branches may lower the energy of the first excited state. However, there is no obvious change in absorption spectra when the solvent was changed from toluene to DMF in the order of increasing polarity, except for ST-G2 in DMF. Notice that the offset between DMF and THF decreases from ST-G1 to ST-G1.5, implying that the solvent effect³⁴ does not play a dominant role. Therefore, the combination of solvent effect and interaction among branches makes the absorption spectra complicated.

One-photon fluorescence spectra show features similar to those of absorption spectra. Peak wavelengths are at wavelengths of 449, 458, and 475 nm for ST-G1, ST-G1.5, and ST-G2 in THF, respectively. As mentioned above, the red-shift of the absorption peak is ascribed to the strong interaction among chromophores. It is well-known that DMF has the largest polarity among the three solvents, toluene has the lowest polarity, and the THF is intermediate. The red-shift of the fluorescence peak with the increasing polarity of solvent reflects that the energy level responsible for fluorescence emission is localized on the ICT state²⁰ and there is a significant difference of polarity between the ground state and the ICT state.

3.2 Two-Photon Fluorescence Spectra (TPF). Under the excitation of 800 nm pulses with a pulse duration of 140 fs, all three sample solutions in THF emit intense frequency up-converted fluorescence. Figure 3 shows TPF spectra of three molecules under different pump intensities. The blue fluorescence could even be observed under excitation of unfocused laser pulses with pulse energy of several microjoules for ST-G1. From the insets, we see good linear dependence of fluorescence intensity on the square of the excitation intensity. Combined with absorption spectra, it provides reliable evidence that the fluorescence emission originates from the TPA process. The fluorescence peaks are located at 460, 481, and 488 nm for ST-G1, ST-G1.5, and ST-G2, respectively. In comparison

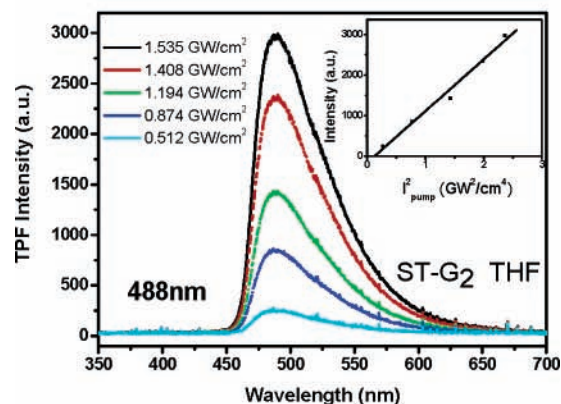
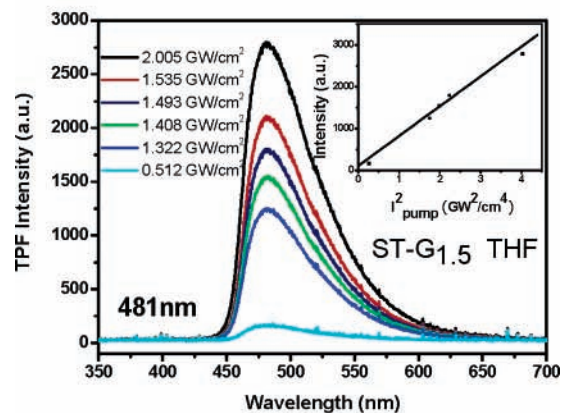
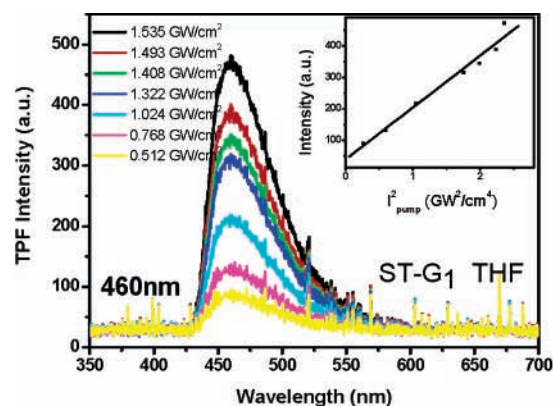


Figure 3. Two-photon fluorescence spectra of three molecules in THF pumped by femtosecond laser pulses at 800 nm at different incident power intensities; inset shows the linear dependence of TPF intensity on the square of the excitation intensity.

with one-photon fluorescence spectra, their peak wavelengths are red-shifted about 10–20 nm in THF. The red-shift can be explained by the reabsorption effect, as we used solutions with a much higher concentration in the TPF experiment.³⁵

3.3. Nonlinear Transmission Measurement. TPA cross sections of three molecules were determined by the femtosecond open-aperture z-scan technique at 800 nm. The values of the two-photon absorption coefficient (β) were determined by fitting the experimental results using a self-compiled program. The TPA cross section can be calculated from the formula $\sigma = h\nu\beta/$

TABLE 1: Photophysical Properties of Samples in Different Solvents

	$\lambda_{\max}^{\text{ab}}$ (nm)			$\lambda_{\max}^{\text{pl}}$ (nm)			σ_2 (GM)		
	DMF	THF	toluene	DMF	THF	toluene	DMF	THF	toluene
ST-G1	373	368	377	461	449	445	43 ± 3	41 ± 2	40 ± 2
ST-G1.5	393	390	379	482	458	443	125 ± 6	81 ± 4	58 ± 3
ST-G2	385	401	405	445	475	452	280 ± 10	188 ± 8	101 ± 5

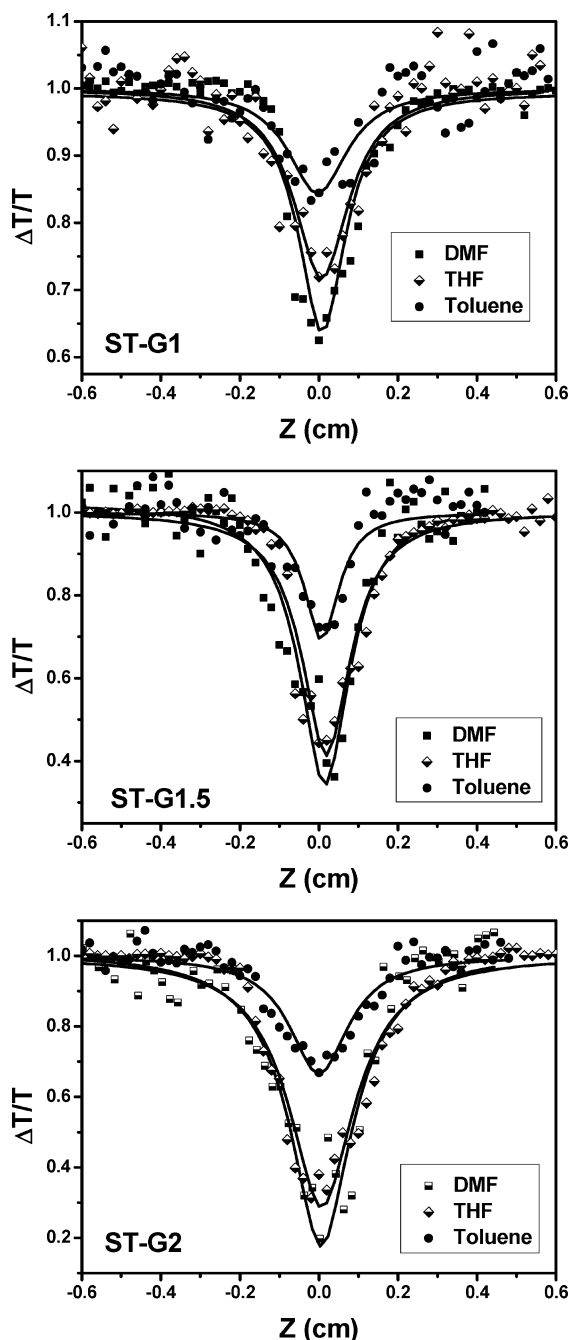


Figure 4. Open-aperture z-scan profiles for molecules in three solvents: DMF, THF, and toluene.

$N_0 = 10^3 h\nu\beta/N_A C$, where N_0 is the number density of absorption centers, N_A is the Avogadro constant, and C represents the solute molar concentration. Figure 4 shows the open-aperture z-scan results of ST-G1, ST-G1.5, and ST-G2 in three solvents, and the calculated values are summarized in Table 1. Though the decrease of the normalized transmission at the valley of open z-scan curves for ST-G1.5 and ST-G2 in DMF are slightly larger than those in THF, on the basis of the treatment of the data, large differences in their TPA cross sections (more than a factor of 1.5) were found. We note that the TPA cross section increases in the order of ST-G1, ST-G1.5, and ST-G2 in the same solvent. Take toluene solution as an example; for the smallest molecule ST-G1, its TPA value is about 40 GM. As the molecule enlarges, the TPA value increases significantly. For ST-G2 with the largest generation number as well as the most chromophores, the calculated TPA value is as much as 101 GM. When the

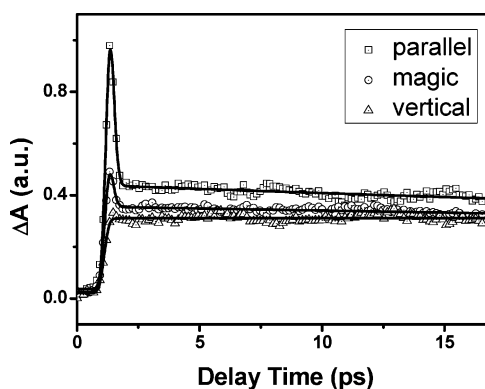


Figure 5. Degenerate pump-probe dynamics for ST-G2 in THF at 800 nm under three polarization configurations: parallel, perpendicular, and magic-angle.

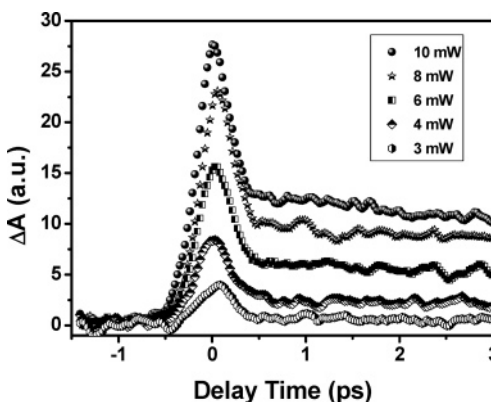


Figure 6. Degenerate pump-probe dynamics for ST-G2 at different excitation powers.

solvent was changed from toluene to DMF, TPA values increased. It is known that forming D- π -A and D- π -D structures is very effective in improving the TPA property³⁶ due to the increasing delocalization of the electron cloud which makes electron-transfer much easier. It was claimed that the TPA cross section increases in proportion to N^2 , where N denotes the number of triphenylamine groups in multibranch molecules.¹⁹ However, the relationship seems appropriate only in the case for THF solutions of our samples. All three compounds are triphenylamines joined through ethenyl which is very similar to the structure they reported, and the sum of triphenylamines is equal to 2, 4, and 6 for ST-G1, ST-G1.5, and ST-G2, respectively. The values of the TPA cross section in THF are 41, 81, and 188 GM, which nearly obey the rule of TPA cross section $\propto N^2$ scaling, 1:3:5 proportion in our multibranch systems.

Second, comparing TPA values of the same compound in different solvents, we found that the TPA value increases with an increase of solvent polarity. DMF has the largest polarity among the three solvents; therefore, the TPA value is greatly enlarged to 280 GM for ST-G2 in DMF. If the solvent was changed to THF, the value decreased to 188 GM. When ST-G2 was dissolved in toluene, whose polarity is quite small, the TPA value is only a little more than one-third of its DMF solution. However, there seems to be no big difference for ST-G1 in all three solvents. Luo has done some calculations on the relationship between the TPA value and the polarity of the solvent.³⁷ He showed that at the beginning, the TPA value increases along with the rising of the polarity of solvents; when the polarity is large enough, the TPA value will not increase any longer. That is to say, the influence of the solvent effect imposed on TPA cross section has a basic precondition that

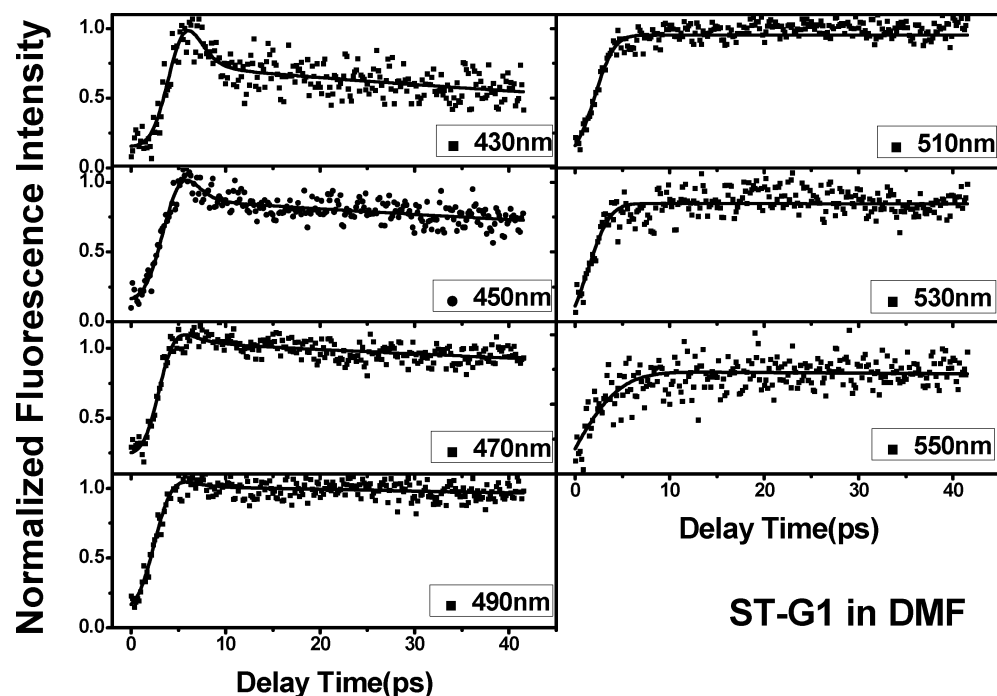


Figure 7. Fluorescence decay dynamics of ST-G1 at different detection wavelengths under excitation at 400 nm.

the polarity of solvent should be in a certain range. Beyond this range, the effect will not be remarkable and the TPA value will fix on a stationary number. For ST-G1.5 and ST-G2, the TPA value increases continuously as the solvent was changed from toluene, to THF, and to DMF, indicating that these samples show a great potential for enhancing the TPA value when dissolved in a solvent with a large dipole moment. Woo et al. also reported similar results obtained by TPF measurement that the sample dissolved in a solvent with a large dipole moment shows a larger TPA cross section.³⁸ Their centrosymmetric compound named 8N showed a TPA value of 910 GM in toluene, and when the solvent was changed to THF, the value was enhanced by a factor of 1.7 which is similar to that of ST-G2 whose TPA value was enhanced by a factor of 1.8. The TPA value is dependent on the dipole moment of the ground state, excited state, and the transition dipole moment, and all of these factors will be remarkably changed in different solvents, inducing diversity of measured TPA values.

Besides, the greatest enhancement appeared to be 7-fold for ST-G2 to ST-G1 in DMF, indicating the strong interaction among chromophores. From ST-G1 to ST-G1.5, the number of triphenylamine units is increased by 2 and the increment is 40 GM in THF. However, the number of triphenylamine units in ST-G2 is two times larger than that in ST-G1.5, and the increment is more than 100 GM. Similar phenomena were observed in other solvents also. This is attributed to the variation of the coupling strength between chromophores in the molecules with different generation numbers. Because ST-G2 possesses the most triphenylamines and corresponding strongest interaction among branches, the TPA magnification is the most prominent among the three molecules. It could also be deduced that the solvent effect mainly affects the interaction.

3.4. Femtosecond Pump–Probe Measurement. As mentioned above, ST-G2 showed the largest TPA cross section in comparison with others under the same conditions. It is evident that the generation number does play a key role in determining the TPA cross section of these chromophores. To better understand the dynamics of the excited state, ultrafast pump–probe experiments were carried out. We performed degenerate

TABLE 2: Fitting Constants of TRPL Results for ST-G1 in DMF

G1, DMF	$\tau_1(\text{ps})/A1$	$\tau_2(\text{ps})/A2$	risetime (ps)
430 nm	5.6/0.5	> 1000/0.4	2.4
450 nm	6.1/0.34	> 1000/0.6	3.2
470 nm	13.8/0.1	> 1000/0.6	3.5
490 nm	> 1000 ps		5
510 nm	> 1000 ps		5.5
530 nm	> 1000 ps		6
550 nm	> 1000 ps		8

pump–probe experiments at 800 nm with parallel, perpendicular, and magic-angle polarization configurations. Shown in Figure 5 are the pump–probe data together with fitting curves. Though all curves show transient absorption signals, which means that the excited state has a larger absorption cross section than that of ground state, very different features were observed for the three samples. When the pump and probe beams were in parallel polarization, there is a sharp absorption signal whose time scale is similar to that of the pulse duration. However, the peak totally disappeared if the probe beam polarization was adjusted to be perpendicular to the pump beam. We ascribe this ultrafast peak to the possible coherent artifacts. Subsequent decays are attributed to the relaxation of the ICT state.³⁹ Figure 6 shows the transient profiles of parallel pump–probe experiments for ST-G2 in THF under a variety of excitation intensities. As the excitation power decreases, all transient curves exhibit a similar shape. The ultrafast sharp signal finishes in about 500 fs, and the subsequent decay process reflects a relatively long time of the ICT state. The evolution of the ICT state which is accompanied by fluorescence emission usually is completed in hundreds of picoseconds; this will be discussed in the TRFL section.

3.5. Time-Resolved Fluorescence Measurement. By using an OKG setup, two of these samples, ST-G1 and ST-G2, were chosen for our study of the dynamics of excited states which are responsible for the evolution of the fluorescence emission. Here we selected DMF as the solvent because it has the strongest polarity. Shown in Figure 7 are the normalized TRFL results

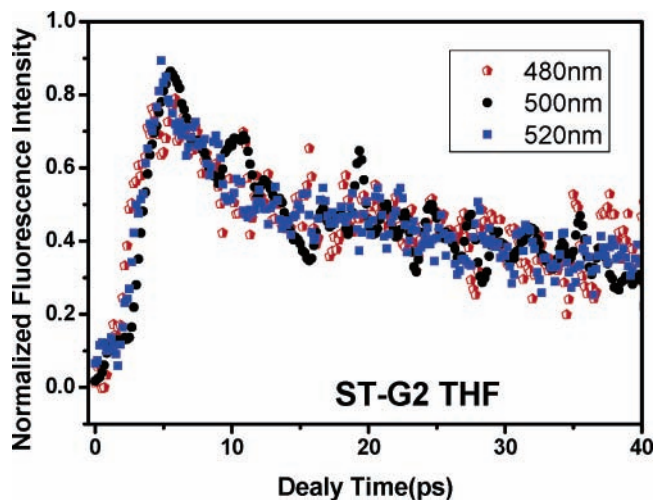


Figure 8. Fluorescence decay of ST-G2 measured at three detection wavelengths under excitation at 400 nm.

for ST-G1 in DMF, and we see a substantial rising-time component whose dynamics are strongly wavelength-dependent. The fit to experimental data could be accomplished by use of a multiexponential expression. The fitting data are summarized in Table 2. The rising time was found to be 2.4 ps at 430 nm, and it increases gradually with the increase of the wavelength. When the detecting wavelength was tuned to 550 nm, the rising time was prolonged to 8 ps. This gives an indication of the establishing processes of the population in the different excited states relating to fluorescence emission. The rising time reflects the accumulation of the population of the ICT state.²⁰ The formation of ICT for ST-G1 should be reasonably accompanied by a charge-transfer process which is accomplished in about 2.4 ps. In ST-G1, the two triphenylamines flanking both sides serve as donors and join together to form a D- π -D structure through ethylene. Once the molecule is excited, the initial excitation may locate on an individual chromophore, after that it begins delocalizing. When the charge-transfer process is completed, the ICT state starts the relaxation to TICT (twisted ICT). We can clearly see that when detecting wavelengths are at 430, 450, or 470 nm, there are two decay routes for the population in the excited state: one is the relaxation to the lower levels of the ICT state and the other is direct relaxation to the ground state accompanied by emission of a photon. When the wavelength is tuned to the red side, the ratio between two routes is getting smaller, as the first route becomes negligible due to the fact that there are few levels lower than the detected state. That is why the dynamic curves exhibit only one decay process at wavelengths of 490, 510, 530, and 550 nm. The relatively long decay process is a reflection of the evolution process of the ICT state which is far beyond our time window, hence we cannot get the exact lifetime of that state.

For ST-G2, when the detecting wavelength was tuned from 480 to 520 nm which are around the TPF peak, their dynamics characters did not show an obvious difference, as shown in Figure 8. All three curves exhibited a fast decay with a lifetime of about 10 ps and another relatively long process. Generally speaking, the wavelength-dependent dynamics could be caused by a solvent effect or photoinduced structural transformation. For molecules with D- π -D structure, the polarity of the ICT state is close to that of the ground state, unlike D- π -A structural molecules, especially for ST-G2 which possesses good symmetry. So we exclude the influence of solvent effect. In addition, strong interactions among chromophores may also be a possible reason.

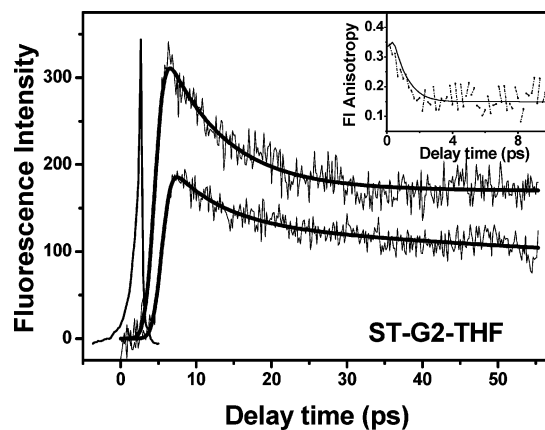


Figure 9. Transient fluorescence dynamics of ST-G2 for parallel and perpendicular polarizations. Inset shows the fluorescence anisotropy decay behavior.

3.6. Time-Resolved Fluorescence Anisotropy Measurement. As we all know, anisotropy can be decided by

$$r(\tau) = \frac{I_{\parallel} - I_{\perp}}{I_{\parallel} + 2I_{\perp}}$$

where I_{\parallel} (I_{\perp}) denotes the fluorescence intensity whose polarization is parallel (perpendicular) to that of the excited beam. However, analyzing TRFL experimental data on the basis of the OKG technique is a great challenge because it is more complicated than the analysis of transient absorption and fluorescence up-conversion experimental data. In the latter, the system response can be simply considered as Gaussian which is convenient for deconvolution treatment. In our experiment, the system response should be the response profile of CS₂. Thus, we used the following two formulas in the calculation:

$$I_{\parallel} = \int \sigma(t - \tau) [A_1 e^{-t/\tau_1} + A_2 e^{-t/\tau_2} + A_3 e^{-t/\tau_3}] [1 + 2\{(r_0 - r_1)e^{-t/\tau_r} + r_1\}] dt$$

$$I_{\perp} = \int \sigma(t - \tau) [A_1 e^{-t/\tau_1} + A_2 e^{-t/\tau_2} + A_3 e^{-t/\tau_3}] [1 - \{(r_0 - r_1)e^{-t/\tau_r} + r_1\}] dt$$

where τ_r is the time constant of anisotropy decay, r_0 and r_1 represent initial value and residual value, respectively, and σ represents the system response.

Anisotropy study is a powerful tool for gaining additional information about the energy redistribution and the dynamics of electronic coupling in multibranch molecules. It has been widely used in experiments on the photosynthetic reaction center.⁴⁰ Recently, Goodson et al. reported plenty of significant results based on time-resolved fluorescence up-conversion measurement on optical dendrimers.^{22,24,29,39,41,42} They proposed that anisotropy shows fast decay and small residual value if there are strong intramolecular interactions among branches.²² They also found that in comparison with the monomer, the dimer and trimer show a shorter depolarization time and lower residual value.²⁹

Figure 9 shows the TRFL anisotropy experimental results of ST-G2 in THF at 480 nm. The initial anisotropy value is 0.34 which is a little smaller than 0.4 (reported in ref 26). An anisotropy decay process with a lifetime of 720 fs is observed. Usually, a large initial anisotropy value and fast decay indicate strong intramolecular interactions which directly affect energy redistributions and generate a large NLO effect.²² This may be

a reason why the measured TPA cross section of ST-G2 is only a half of theirs (600 GM) because their anisotropy decay time is as short as 40 fs.

4. Conclusions

From our measurement we find a significant enhancement in the NLO properties of ST-G2 as compared to that of ST-G1, which is explained in terms of the strong interactions among the chromophores in the branched structure. Z-scan and TPF experiments confirm that the up-converted fluorescence arises from the TPA mechanism without doubt. The solvent effect also plays an important role in improving the NLO effect that as the solvent polarity becomes larger, the TPA cross section increases. A rise time of 2.4 ps in the TRFL experiment is attributed to the energy redistribution among the levels in the excited state. Very different fluorescence relaxation characters are observed between ST-G1 and ST-G2, indicating that a stronger interaction exists in the sample with larger generation numbers (chromophores). Anisotropy kinetics which is regarded as one of the most useful tools in obtaining information of the excited state shows that there is a fast decay for ST-G2 with a time constant of ~ 720 fs. All the obtained results demonstrate that the use of the combination of different ultrafast measurement techniques, including femtosecond z-scan, femtosecond pump-probe, femtosecond two-photon fluorescence, and time-resolved fluorescence, is very useful in exploring the ultrafast response and nonlinear optical properties of new materials. Our research also confirmed that the multibranching chromophore structure is very useful in enhancing the two-photon absorption property, and it has potential in future applications.

Acknowledgment. The authors are grateful to the National Science Foundation of China (Grant Nos.10374020 and 10674031) for financial support of this investigation.

References and Notes

- Zhou, W.; Kuebler, S. M.; Braun, K. L.; Yu, T.; Cammack, J. K.; Ober, C. K.; Perry, J. W.; Marder, S. R. *Science* **2002**, *296*, 1106.
- Kawata, S.; Sun, H.-B.; Tanaka, T.; Takada, K. *Nature* **2001**, *412*, 697.
- Maruo, S.; Nakamura, O.; Kawata, S. *Opt. Lett.* **1997**, *22*, 132.
- Kenk, W.; Strickler, J. H.; Webb, W. W. *Science* **1990**, *248*, 73.
- Larson, D. R.; Zipfel, W. R.; Williams, R. M.; Clark, S. W.; Bruchez, M. R.; Wise, T. W.; Webb, W. W. *Science* **2003**, *300*, 1434.
- He, G. S.; Xu, G. C.; Prasad, P. N.; Reinhardt, B. A.; Bhatt, J. C.; Mckellar, R.; Dillard, A. G. *Opt. Lett.* **1995**, *20*, 435.
- Belfield, K. D.; Schafer, K. J. *Chem. Mater.* **2002**, *14*, 3656.
- Kogej, T.; Beljonne, D.; Meyers, F.; Perry, J. W.; Marder, S. R.; Bredas, J. L. *Chem. Phys. Lett.* **1998**, *298*, 1.
- Kannan, R.; He, G. S.; Yuan, L.; Xu, F.; Prasad, P. N.; Reinhardt, B. A.; Baur, J. W.; Vaia, R. A.; Tan, L. S. *Chem. Mater.* **2001**, *13*, 1896.
- Cho, B. R.; Son, K. H.; Lee, S. H.; Song, Y.-S.; Lee, Y.-K.; Jeon, S.-J.; Choi, J. H.; Lee, H.; Cho, M. *J. Am. Chem. Soc.* **2001**, *123*, 10039.
- Wang, C.-K.; Macak, P.; Luo, Y.; Ågren, H. *J. Chem. Phys.* **2001**, *114*, 9813.
- Porres, L.; Mongin, O.; Katan, C.; Charlot, M.; Pons, T.; Mertz, J.; Blanchard-Desce, M. *Org. Lett.* **2004**, *6*, 47.
- Mongin, O.; Porres, L.; Katan, C.; Pons, T.; Mertz, J.; Blanchard-Desce, M. *Tetrahedron Lett.* **2003**, *44*, 8121.
- Venleton, L.; Moreaus, L.; Mertz, J.; Blanchard-Desce, M. *Chem. Commun.* **1999**, *20*, 2055.
- Lee, H. J.; Sohn, J.; Hwang, J.; Park, S. Y.; Choi, H.; Cha, M. *Chem. Mater.* **2004**, *16*, 456.
- Macak, P.; Luo, Y.; Norman, H.; Ågren, H. *J. Chem. Phys.* **2000**, *113*, 7055.
- Chung, S.-J.; Kim, K.-S.; Lin, T.-C.; He, G. S.; Swiatkiewicz, J.; Prasad, P. N. *J. Phys. Chem. B* **1999**, *103*, 10741.
- Li, B.; Tong, R.; Zhu, R.; Meng, F.; Tian, H.; Qian, S. *J. Phys. Chem. B* **2005**, *109*, 10705.
- Drobizhev, M.; Karotki, A.; Rebane, A.; Spangler, C. W. *Opt. Lett.* **2001**, *14*, 1081.
- Drobizhev, M.; Karotki, A.; Dzenis, Y.; Rebane, A.; Suo, Z.; Spangler, C. W. *J. Phys. Chem. B* **2003**, *107*, 7540.
- Li, B.; Tong, R.; Zhu, R.; Meng, F.; Tian, H.; Qian, S. *J. Phys. Chem. B* **2005**, *109*, 10705.
- Drobizhev, M.; Rebane, A.; Suo, Z.; Spangler, C. W. *J. Lumin.* **2005**, *111*, 291.
- Varnavski, O. P.; Ostrowski, J. C.; Sukhomlinova, L.; Twieg, R. J.; Bazan, G. C.; Goodson, T., III. *J. Am. Chem. Soc.* **2002**, *124*, 1736.
- Katan, C.; Terenziani, T.; Mongin, O.; Werts, M. H. V.; Porres, L.; Pons, T.; Mertz, J.; Tretiak, S.; Blanchard-Desce, M. *J. Phys. Chem. A* **2005**, *109*, 3024.
- Goodson, T., III. *Acc. Chem. Res.* **2005**, *38*, 99.
- Lahankar, A. S.; West, R.; Barnavski, O.; Xie, X.; Goodson, T., III; Sukhomlinova, L.; Twieg, R. *J. Chem. Phys.* **2004**, *120*, 337.
- Varnavski, O.; Samuel, I. D. W.; Palsson, L.-O.; Beavington, R.; Burn, P. L.; Goodson, T., III. *J. Chem. Phys.* **2002**, *116*, 8893.
- Wang, Y.; Ranasinghe, M. I.; Goodson, T., III. *J. Am. Chem. Phys.* **2003**, *125*, 8562.
- Varnavski, O.; Goodson, T., III; Sukhomlinova, L.; Twieg, R. *J. Phys. Chem. B* **2004**, *108*, 10484.
- Wang, Y.; He, G. S.; Prasad, P. N.; Goodson, T., III. *J. Am. Chem. Soc.* **2005**, *127*, 10128.
- Zhonghua, P.; Melinger, J. S.; Kleiman, B. *Photosynth. Res.* **2006**, *87*, 115.
- Wang, X.; Yang, P.; Li, B.; Jiang, W.; Huang, W.; Qian, S.; Tao, X.; Jiang, M. *Chem. Phys. Lett.* **2006**, *424*, 333.
- Sheik-Bahae, M.; Said, A. A.; Van Stryland, E. W. *Opt. Lett.* **1989**, *14*, 955.
- Takeda, J.; Nakajima, K.; Kurita, S.; Tomimoto, S.; Saito, S.; Suemoto, T. *Phys. Rev. B* **2000**, *62*, 10083.
- Sharma, A.; Schulman, S. G. *Introduction to Fluorescence Spectroscopy*; Wiley-Interscience: New York, 1999.
- Wu, L.-Z.; Tang, X.-J.; Jiang, M.-H.; Tung, C.-H. *Chem. Phys. Lett.* **1999**, *315*, 379.
- Albota, M.; Beljonne, D.; Bredas, J.-L.; Ehrlich, J. E.; Fu, J.-Y.; Heikal, A. A.; Hess, S. E.; Kogej, T.; Levin, M. D.; Marder, S. R.; McCrod-Maughon, D.; Perry, J. W.; Rumi, H. R.; Subramaniam, G.; Webb, W. W.; Wu, X.-L.; Xu, C. *Science* **1998**, *181*, 1653.
- Luo, Y.; Norman, P.; Macak, P.; Ågren, H. *J. Phys. Chem. A* **2000**, *104*, 4718.
- Woo, H. Y.; Liu, B.; Kohler, B.; Korystov, D.; Mikhailovsky, A.; Bazan, G. C. *J. Am. Chem. Soc.* **2005**, *127*, 14721.
- Bhaskar, A.; Bamakrishna, G.; Zu, Z.; Twieg, R.; Hales, J. M.; Hagan, D. J.; Stryland, E. V.; Goodson, T., III. *J. Am. Chem. Soc.* **2006**, *128*, 11840.
- Arentt, D. C.; Moser, C. C.; Dutton, P. L.; Scherer, N. F. *J. Phys. Chem. B* **1999**, *103*, 2014.
- Wang, Y.; Ranasinghe, M. I.; Goodson, T., III. *J. Am. Chem. Soc.* **2003**, *125*, 9562.
- Ranasinghe, M. I.; Wang, Y.; Goodson, T., III. *J. Am. Chem. Soc.* **2003**, *125*, 5258.